Available online at www.sciencedirect.com
ScienceDirect
Trans. Nonferrous Met. Soc. China 31(2021) 416−425
Transactions of Nonferrous Metals Society of China
www.tnmsc.cn

Microstructure and mechanical properties of TC4 titanium alloy K-TIG welded joints

Shu-wan CUI[1,2], Yong-hua SHI[2], Cheng-shi ZHANG[3]

1. School of Mechanical and Transportation Engineering, Guangxi University of Science and Technology, Liuzhou 545006, China;
2. School of Mechanical and Automotive Engineering, South China University of Technology, Guangzhou 510640, China;
3. SAIC Liuzhou Automobile Transmission Co., Ltd., Liuzhou 545006, China

Received 21 March 2020; accepted 23 December 2020

Abstract: The 12 mm-thick Ti−6Al−4V (TC4) titanium alloy plates were welded using keyhole tungsten inert gas (K-TIG) welding at various heat inputs. The microstructure, grain boundary (GB) characteristics and mechanical properties of the weld metal zone (WMZ) were analyzed. The test results show that the K-TIG welds are well formed, and no obvious defects are observed when the heat input is 2.30−2.62 kJ/mm. When the heat input gradually increases, α laths increase in length, and α' phase and residual β phase are reduced. The electron backscatter diffraction (EBSD) test results indicate that the high-angle GB proportion in the WMZ increases with the increase of heat input. The tensile strength of the WMZ gradually decreases and the elongation of the WMZ increases when the heat input increases from 2.30 to 2.62 kJ/mm. The impact toughness of the WMZ increases as the heat input increases.
Key words: K-TIG welding; heat input; α' phase; high-angle grain boundary; Charpy impact fracture surface

1 Introduction

The Ti−6Al−4V (TC4) titanium alloy is a very important structural material and is currently widely used in the field of marine engineering [1−3]. For example, it is widely used in the hull construction of condensate tankers. CUI et al [4] reported that the TC4 titanium alloy was a two-phase titanium alloy comprising the α+β phases and had the advantages of low density, high strength and high corrosion resistance. Welding is an indispensable process technology in the processing and manufacturing of titanium alloys. Titanium alloys had a strong activity in the molten state, and they reacted readily with various substances during welding, which deteriorated the performance of the welded joints, as reported by DING and GUO [5]. Keyhole tungsten inert gas (K-TIG) welding is a TIG welding method with keyhole mode. In contrast to TIG welding, it can weld titanium alloy plates that are less than 16 mm in thickness in a single-pass welding without filling the welding metal or opening the groove [6]. The heat-affected zone (HAZ) of the K-TIG welded joint is relatively narrow, and the welding deformation is relatively small [7,8]. Therefore, K-TIG welding enables double-sided forming of single-sided welding. For a certain thickness of TC4 titanium alloy, K-TIG welding can save welding metal, improve welding efficiency and reduce cost. CUI et al [4] also pointed out that K-TIG welding was a very economical method for welding medium-thick TC4 titanium alloys. However, during the welding

Corresponding author: Yong-hua SHI; Tel/Fax: +86-20-87114407; Mobile: +86-13539914820; E-mail: yhuashi@scut.edu.cn
DOI: 10.1016/S1003-6326(21)65506-1

thermal cycle, the microstructure of the titanium alloy welded joint has undergone significant changes, which has a certain impact on the mechanical properties of the welded joint. Therefore, it is very important to study the microstructure of titanium alloy welded joints.

At present, researchers have studied the microstructure of titanium alloy welded joints with different welding methods. WANG et al [9] discussed the microstructure and mechanical properties of TC4 titanium alloy electron beam welded joints. They reported that the inhomogeneity of microstructure in the welded joint was formed due to different microstructures of base metal (BM). LATHABAI et al [10] welded commercially pure titanium with K-TIG welding. They proved that 4 mm/s was the best choice for the welding speed of commercially pure titanium workpieces with a thickness of 12.7 mm. ROSELLINI and JARVIS [11] also used the K-TIG welding method to weld titanium alloy tubes. They showed that the mechanical properties of the K-TIG weld metal zone (WMZ), such as the tensile properties, impact properties and microhardness values, were almost the same as those of conventional TIG WMZ. CUI et al [4] welded 12 mm-thick TC4 plates by using K-TIG welding. They studied the microstructure and texture of the BM, HAZ and WMZ of TC4 K-TIG welded joints. SQUILLACE et al [12] indicated that during the welding thermal cycle, the microstructure of TC4 titanium alloy welded joints changed significantly. Microstructural changes are needed to improve the tensile properties and impact properties of K-TIG welded joints. However, during the K-TIG welding process, heat input has a certain influence on the mechanical properties and microstructure of the TC4 titanium alloy K-TIG WMZ, and research on this topic is limited. In this work, TC4 titanium alloy plates were welded with various heat inputs by the K-TIG welding system. During the K-TIG welding process, filling metals or preparing groove before welding can be avoided. The evolution law of the microstructure and GB characteristics of the K-TIG WMZ under different welding heat inputs were studied. The influencing mechanism of the microstructure and GB characteristics on the mechanical properties of the titanium alloy K-TIG WMZ were analyzed.

2 Experimental

For the K-TIG welding tests, the BM was 12 mm-thick TC4 titanium alloy plate. The dimensions of the TC4 titanium alloy plate were 300 mm × 100 mm. The chemical composition of the TC4 titanium alloy is displayed in Table 1. Figure 1 shows the schematic diagram of the K-TIG welding system. A certain error occurred after the workpieces were cut or mechanically cleaned, so the gap between the two workpieces cannot be guaranteed to be 0 mm. In order to ensure the accuracy of the welding test, two workpieces were fixed with a gap of 0.5 mm before welding. Because TC4 titanium alloy has strong metal activity, it is easily contaminated by oil and other substances, and it oxidizes readily during welding. To obtain high-quality TC4 welds, the workpieces were cleaned with acetone, and the front and back of the workpieces were protected by high-purity argon (99.9%). At a welding speed of 3.5 mm/s, gas flow rate of 20 L/min and electrode gap of 2.0 mm, only the welding current was changed to carry out five sets of tests, referred to as No. 1 to No. 5. The specific welding parameters in the K-TIG experiments are shown in Table 2.

Table 1 Chemical composition of TC4 titanium alloy (BM) plate (wt.%)

Al	V	Fe	C	N	O	H	Ti
6.11	4.06	0.12	0.012	0.012	0.156	0.0015	Bal.

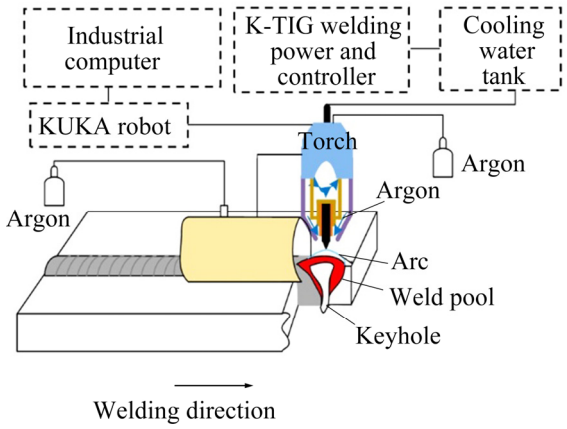

Fig. 1 Schematic diagram of K-TIG welding system

After K-TIG welding, the K-TIG weld geometry profiles were observed. The transverse

cross-sections of TC4 K-TIG welded joints were etched by Keller reagent (2 mL HF+10 mL HNO_3+ 88 mL H_2O). According to the ASTM E709—08 standard, X-ray nondestructive tests (NDTs) were carried out to analyze the defects in the K-TIG welds [13].

Table 2 Welding parameters in K-TIG welding experiments

Test No.	Welding current/ A	Welding speed/ ($mm \cdot s^{-1}$)	Arc voltage/ V	Heat input/ ($kJ \cdot mm^{-1}$)
1	490	3.5	17.0	2.14
2	510	3.5	17.5	2.30
3	530	3.5	18.0	2.45
4	550	3.5	18.5	2.62
5	570	3.5	19.0	2.78

The electron backscatter diffraction (EBSD) technique was applied to characterizing the grain boundary misorientation angle distribution (GBMAD) of the BM and WMZ under varying heat inputs. The specimens for the tensile property test, including the BM and WMZ, were prepared in accordance with the ASTM E8 standard [14]. The specimens for the Charpy impact test, including the BM and WMZ, were prepared in accordance with the ASTM A370 standard [15]. The specimen dimensions for tensile test and Charpy impact test are shown in Fig. 2. The morphologies of the Charpy impact fracture were observed by scanning electron microscopy (SEM).

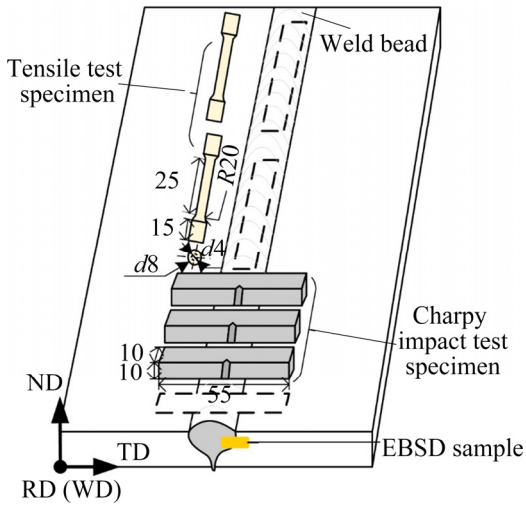

Fig. 2 Specimen dimensions for tensile test and Charpy impact test (unit: mm)

3 Results and discussion

3.1 Effect of heat input on K-TIG weld morphology

Figure 3 shows the transverse cross-sections of the TC4 titanium alloy K-TIG welded joints under various heat input conditions. In Fig. 3(a), it can be seen that the K-TIG weld is not completely penetrated when the heat input is 2.14 kJ/mm. When the heat inputs are 2.30, 2.45 and 2.62 kJ/mm, the TC4 K-TIG welds are completely penetrated. The weld seam collapses, and the reinforcement on the back of the weld is too large when the heat input increases to 2.78 kJ/mm, as shown in Fig. 3(e). This is mainly because when the heat input is relatively

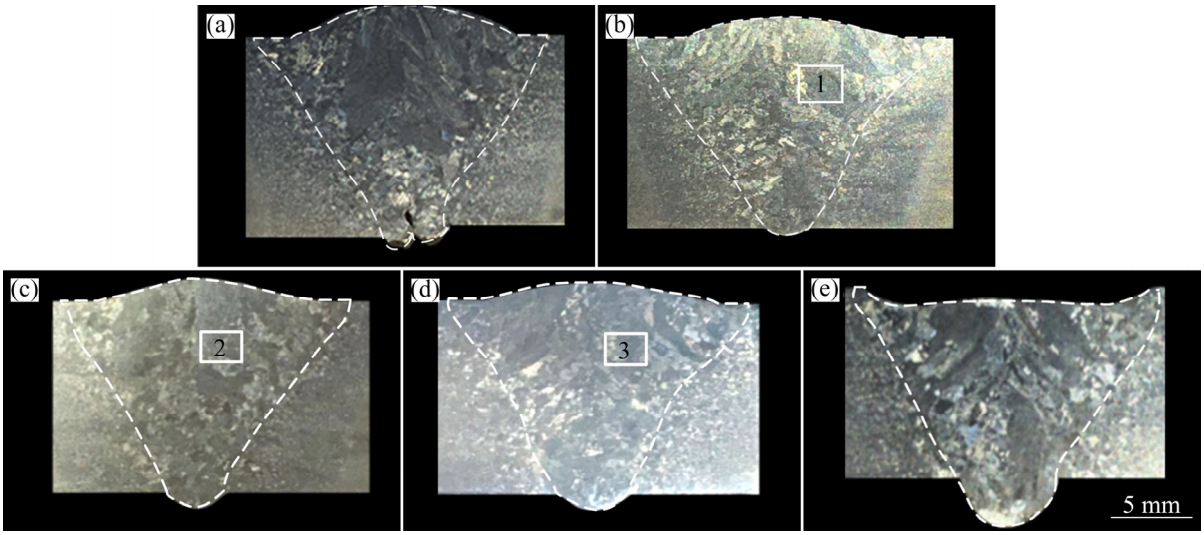

Fig. 3 Transverse cross-sections of K-TIG TC4 titanium alloy welded joint at various heat inputs: (a) 2.14 kJ/mm; (b) 2.30 kJ/mm; (c) 2.45 kJ/mm; (d) 2.62 kJ/mm; (e) 2.78 kJ/mm

small, the penetration of the arc is insufficient. The gas in the molten pool cannot escape from the keyhole in time, so the hole appears in the weld. However, when the heat input is too large, additional metal is melted, and the reinforcement on the back of the weld is too large, so the weld shape is poor. This proves that the K-TIG weld joints at heat inputs of 2.14 and 2.78 kJ/mm do not meet the welding requirements. Therefore, this study focused on the microstructure and mechanical properties of the WMZ when the welding heat inputs were between 2.30 and 2.62 kJ/mm.

Figure 4 displays the profiles of the K-TIG welds at various heat inputs (2.30−2.62 kJ/mm). All of them were well formed, and the welds surfaces were bright and clear. When the heat inputs were 2.30−2.62 kJ/mm, X-ray nondestructive testing photos of the welds were taken. The welds in the picture were uniform, had a light black broadband, and did not have large white spots or lines, which indicated good welds. There were no defects, such as pores or cracks. Combining Fig. 3 and Fig. 4, it was proved that when TC4 titanium alloy plates were welded by using K-TIG welding, the welding process window was relatively small. Therefore, welding heat input is a key factor affecting the performance and morphology of welded joints.

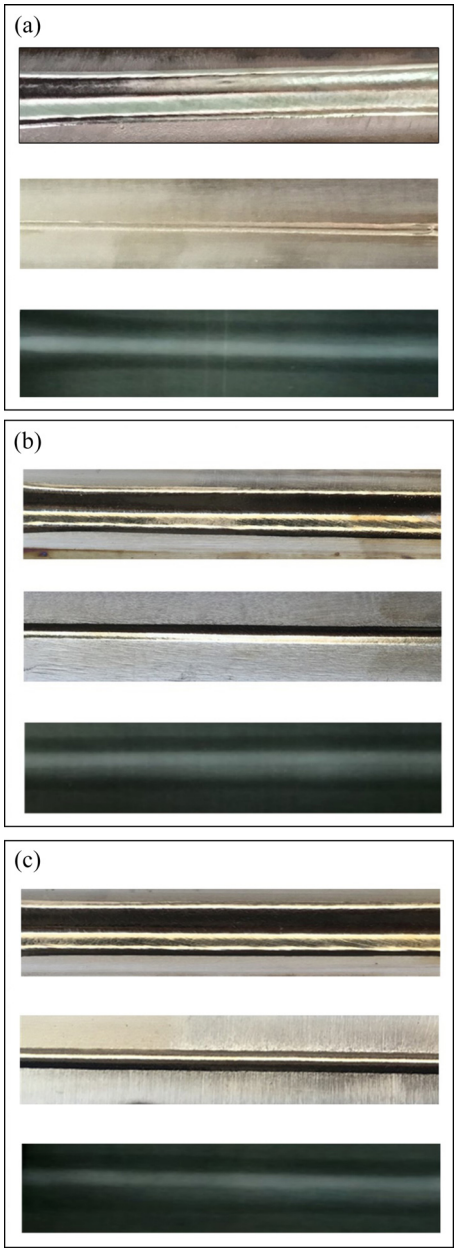

Fig. 4 Profiles of K-TIG welds at various heat inputs: (a) 2.30 kJ/mm; (b) 2.45 kJ/mm; (c) 2.62 kJ/mm

3.2 Microstructure of K-TIG WMZ at various heat inputs

The EBSD technique was used to characterize the microstructure of the BM and WMZ at various heat inputs. Figures 5 and 6 display the phase maps and band contrast images, respectively. The blue phase represents α titanium, and the yellow phase represents β titanium.

Referring to Figs. 5 and 6, the microstructure of the BM was mainly composed of equiaxed α grains, α laths and a few retained β grains. Through Fig. 3, it can be seen that the grains of the WMZ became coarser. Figures 6(b), (c) and (d) display the microstructures of Areas 1, 2 and 3 in Fig. 3, respectively. Compared with the microstructure of the BM, the microstructures of the WMZ at various heat inputs were mainly composed of α laths that were relatively dispersed and distributed in multiple directions. This was mainly because the temperature of the WMZ reached the β transus temperature (995 °C), the primary α grains in the WMZ were completely transformed into β phase, and a large number of α laths formed during the subsequent cooling process. Although the phases in the WMZ were the same at various heat inputs, their morphologies were different. When the heat input was 2.30 kJ/mm, α laths formed in the WMZ were relatively short. When the heat input increased, α laths became long. AHMED and RACK [16] reported that the cooling rate during the $\alpha \rightarrow \beta$ transformation could directly determine the subsequent evolution of the microstructure. When the cooling rate was relatively fast, β phase was directly transformed into α' phase, and residual β phase also existed around α' phase [1]. It could be

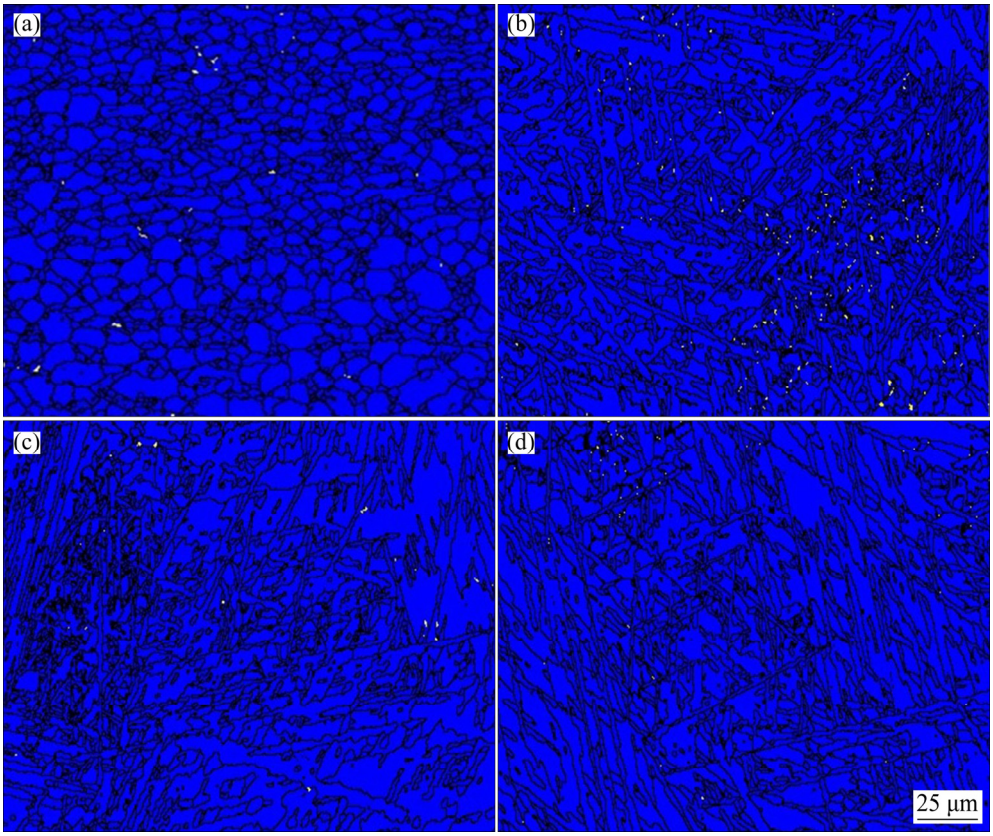

Fig. 5 Microstructures of BM (a) and WMZ at heat inputs of 2.30 kJ/mm (b), 2.45 kJ/mm (c) and 2.62 kJ/mm (d)

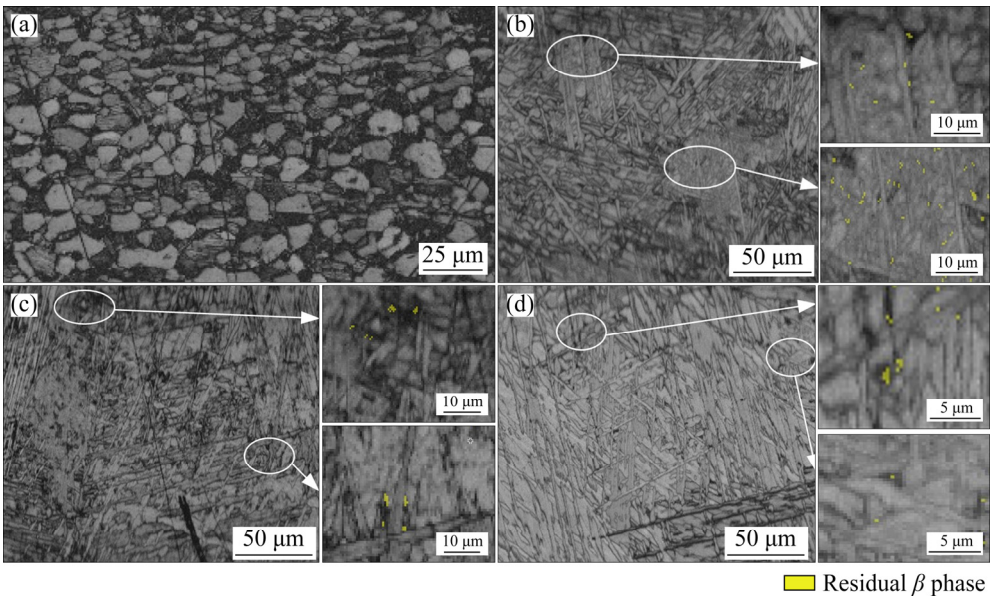

Fig. 6 Band contrast images of BM (a) and WMZ at heat inputs of 2.30 kJ/mm (b), 2.45 kJ/mm (c) and 2.62 kJ/mm (d)

seen from Figs. 6(b−d) that rod-like or granular structures were distributed between α laths. Residual β phase also existed around these structures. Because the K-TIG welding speed was relatively fast and its cooling speed was also fast, it was determined that these rod-like or granular structures in the WMZ comprised α' phase. When the heat input increased, the corresponding cooling rate decreased, and the time for the growth of α laths was sufficient enough. Therefore, when the heat input increased, α laths increased in length, and α' phase and residual β phase were also reduced.

The microstructures of WMZ under varying heat input conditions indicate that only α phase, α' phase and residual β phase exist in the WMZ, and no other precipitated phases exist.

3.3 GBMAD of WMZ at various heat inputs

In polycrystalline materials, the GBMAD has certain influence on the mechanical properties of materials, which was proven by PARK et al [17]. The GBMAD can be categorized as low-angle GB ($2°\leq\theta\leq10°$) and high-angle GB ($\theta\geq15°$) in accordance with the orientation angles of the GB [18]. Figure 7 displays the GBMAD maps of α phase in the BM and WMZ at various heat inputs. The blue lines indicate high-angle GB, and the black lines indicate low-angle GB. Figure 8 shows the high-angle GB proportion of α phase in the BM and WMZ. In the BM, the proportion of high-angle GB was 48.1%. In the WMZ, the proportion of high-angle GB increased as the heat input increased; it was 78.9%, 81.4% and 87.2% when the heat input was 2.30, 2.45 and 2.62 kJ/mm, respectively. This was mainly caused by changes in α phase morphology. In the BM, α phase was mainly equiaxed. In the WMZ, α phase existed mainly in the form of laths. When the heat input increased, α laths became fine and long. Therefore, the proportion of high-angle GB in the WMZ increased as the heat input increased.

In previous study [4], it was found that large-angle GB had certain effect on the impact toughness of welded joints. Under certain conditions, as the proportion of high-angle GB increased, the impact toughness of the material gradually increased. It was proved that the proportion of high-angle GB was the main basis for judging the impact toughness of WMZ. Therefore, it could be inferred that when the heat input increased from 2.30 to 2.62 kJ/mm, the impact toughness of the WMZ gradually increased.

3.4 Mechanical properties

3.4.1 Tensile properties

The tensile properties of the BM and WMZ at various heat inputs are shown in Fig. 9. Figure 9(a) shows the tensile curves of the BM and WMZ at various heat inputs, and Fig. 9(b) displays the yield strength and elongation of the BM and WMZ at various heat inputs. The yield strength and elongation of the BM were 1054.5 MPa and 18.3%, respectively. When the heat inputs were 2.30, 2.45 and 2.62 kJ/mm, the tensile strengths of the K-TIG

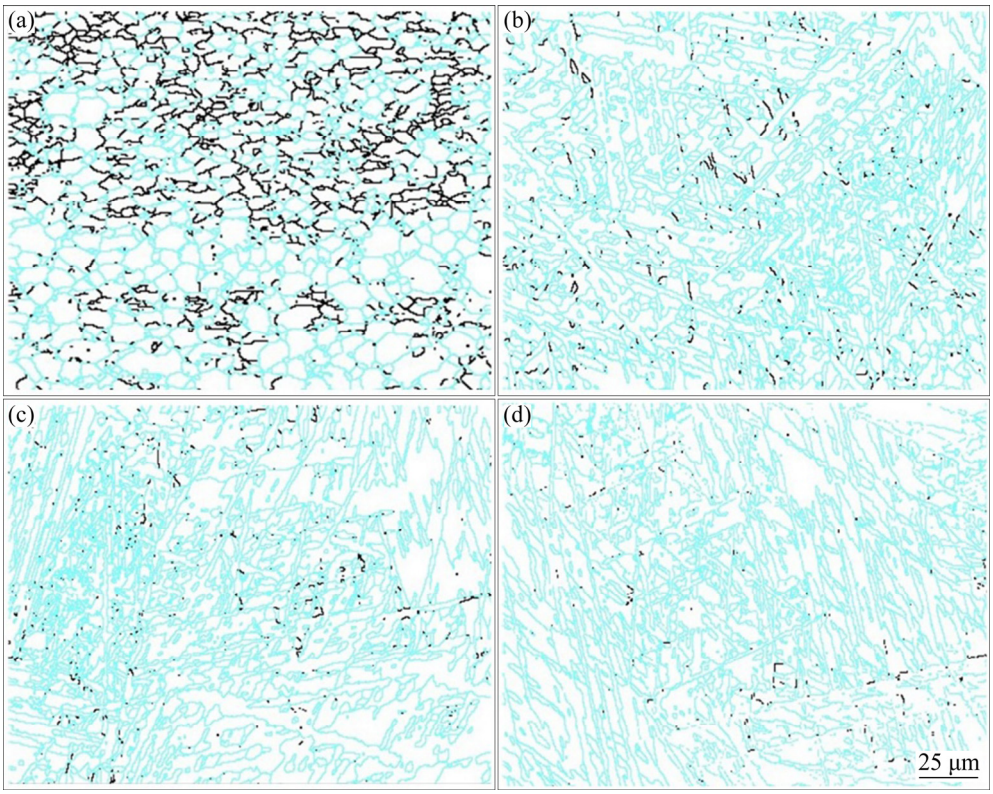

Fig. 7 GBMAD maps of α phase in BM (a) and WMZ at heat inputs of 2.30 kJ/mm (b), 2.45 kJ/mm (c) and 2.62 kJ/mm (d)

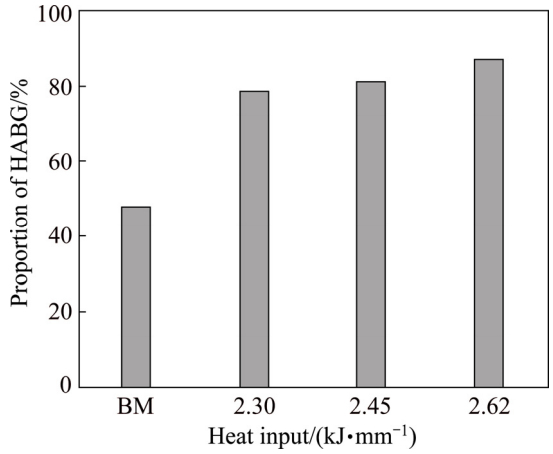

Fig. 8 High-angle GB (HAGB) proportion of α phase in BM and WMZ

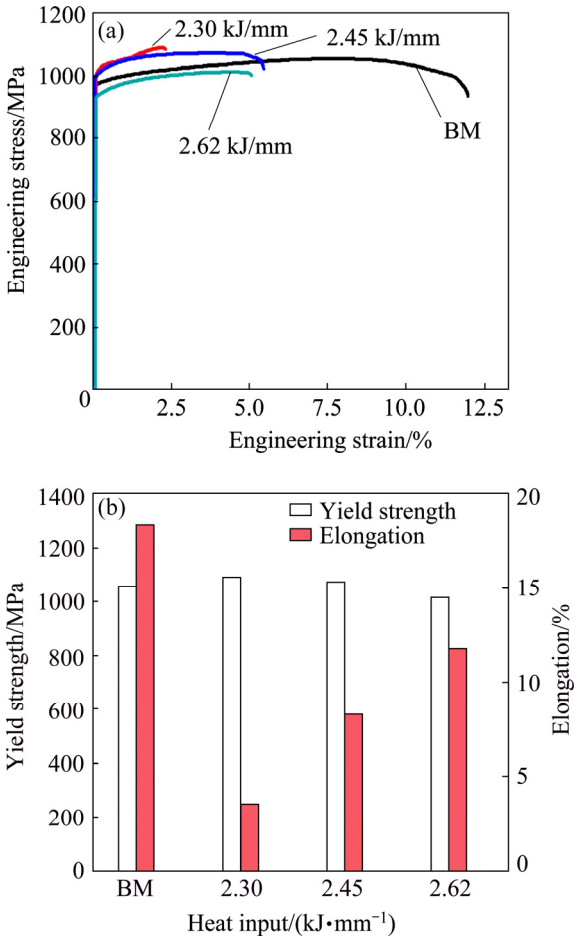

Fig. 9 Engineering stress−engineering strain curves (a), yield strength and elongation (b) of BM and WMZ at various heat inputs

WMZ were 1089.8, 1072.1 and 1013.5 MPa, respectively; the elongations of the K-TIG WMZ were 3.5%, 8.3% and 11.8%, respectively. The experimental results showed that when the heat inputs increased from 2.30 to 2.62 kJ/mm, the tensile strengths of the TC4 titanium alloy K-TIG WMZ gradually decreased. When the heat input was 2.62 kJ/mm, the tensile strength of the WMZ was lower than that of the BM, but the tensile strength requirement (greater than 895 MPa) of the TC4 titanium alloy plate in the ASTM B256—05 standard was reached [19]. The elongation of the TC4 titanium alloy K-TIG WMZ at various heat inputs was lower than that of the BM. When the heat input increased, the elongation of the WMZ gradually increased. This was mainly because α' phase could increase the strength of the material. When the heat input increased, the corresponding cooling rate decreased, and the growth time for the α laths was sufficient enough. The α' phase decreased with increasing heat input, so the tensile strength of WMZ decreased and the elongation of the WMZ increased. By comparing the tensile strength and elongation of the K-TIG WMZ at various heat inputs, it was indicated that the microstructure of the WMZ had a certain effect on its tensile properties. Under certain conditions, the tensile properties of the TC4 titanium alloy K-TIG WMZ could be improved by changing the heat input.

3.4.2 Charpy impact properties

The energies absorbed by the BM and WMZ during the Charpy impact tests are shown in Table 3. When the heat inputs were 2.30, 2.45 and 2.62 kJ/mm, the average values of the energy absorbed in the WMZ were 20.4, 32.1 and 33.6 J, respectively. The average value of the energy absorbed in the BM was 24.3 J. The Charpy impact test results showed that with increasing heat input, the energy absorbed in the WMZ gradually increased. When the heat inputs were 2.45 and 2.62 kJ/mm, the average value of the energy absorbed by the WMZ was larger than that of the BM. When the heat input was 2.30 kJ/mm, the

Table 3 Charpy impact absorbed energy in different zones of specimen

Zone	Heat input/ (kJ·mm^{-1})	Absorbed energy/J			
		No. 1	No. 2	No. 3	Average value
BM	−	23.5	24.2	25.1	24.3
WMZ	2.30	19.9	19.8	21.4	20.4
WMZ	2.45	30.1	33.5	32.7	32.1
WMZ	2.62	33.7	33.7	33.4	33.6

average value of the energy absorbed by the WMZ was slightly lower than that of the BM. However, it reached 84% of the BM.

The fracture micrograph of the BM is displayed in Fig. 10(a). The fracture micrographs of the WMZ at various heat inputs are shown in Figs. 10(b−d). It can be seen that there were tear edges and dimples in the BM and WMZ. Therefore, it can be determined that the BM and WMZ plastically deformed before fracture occurred, and the fracture mode of the WMZ was ductile fracture. It can be seen in Figs. 10(b−d) that when the heat input gradually increased, the dimple size in the impact fracture of the WMZ gradually increased. When the welding heat input increased from 2.30 to 2.62 kJ/mm, the energy absorbed by the WMZ increased during the impact fracture process, which was consistent with the Charpy impact test results. The impact absorbed energy of materials is an important index used to evaluate the anti-destructive ability of metal materials. When other parameters were constant, the greater the value of the impact absorbed energy of the material was, the stronger the impact resistance was and the better the impact toughness was. According to the Charpy impact test results, as the heat input increased, the impact toughness of the K-TIG WMZ also increased.

WRONSKI et al [20] pointed out that high-angle GB could effectively prevent the propagation of brittle crack. Therefore, the higher the proportion of high-angle GB was, the greater the energy absorbed during the fracture process was, and the better the impact toughness was. In Fig. 8, it could be seen that when the heat input was 2.30 kJ/mm, the high-angle GB proportion in the WMZ was greater than that in the BM, while the impact toughness of the WMZ is lower than that of the BM. Therefore, it could be seen that the proportion of high-angle GB was not the only factor affecting the impact toughness. THOMAS et al [21] reported that α' phase had a certain impact on the impact toughness of WMZ. When α' phase appeared in the WMZ, the impact toughness of the WMZ was less than that of the BM. When α' phase was eliminated, the impact toughness of the WMZ was improved. In

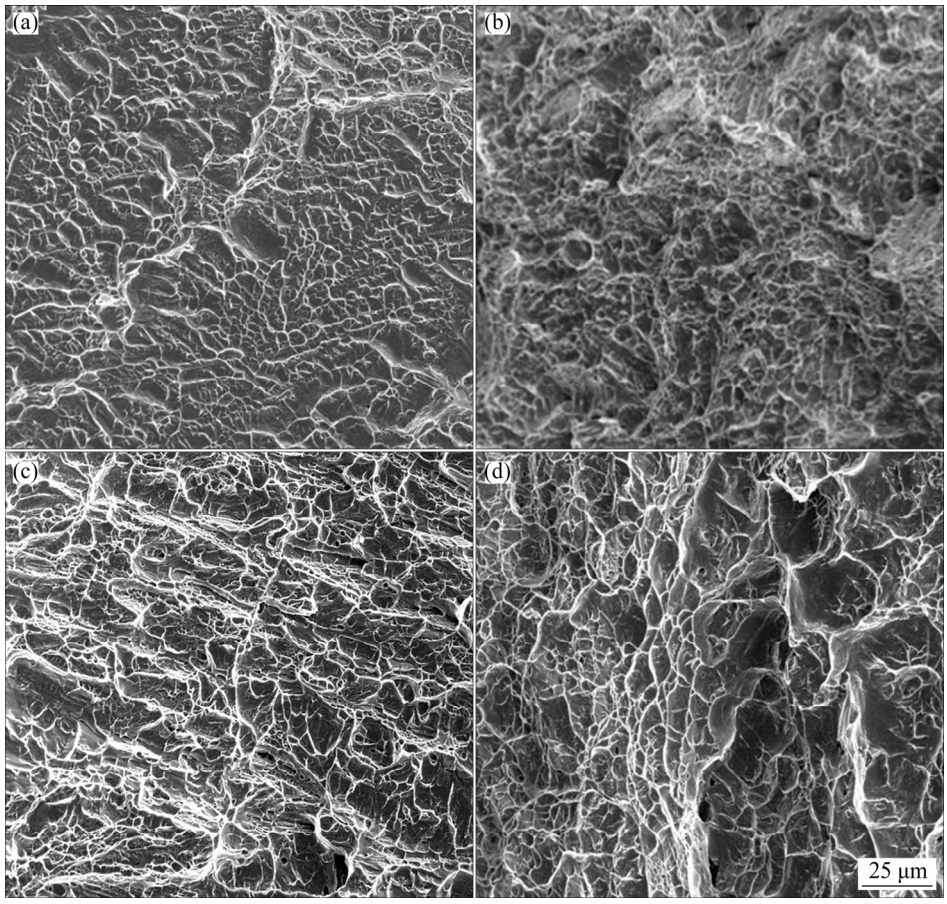

Fig. 10 SEM images of Charpy impact fracture surfaces: (a) BM; (b−d) WMZ at heat inputs of 2.30 kJ/mm (b), 2.45 kJ/mm (c) and 2.62 kJ/mm (d)

Fig. 6, it could be seen that when the heat inputs were 2.30, 2.45 and 2.62 kJ/mm, α' phase appeared in the WMZ. When the heat input was 2.30 kJ/mm, the impact toughness of the WMZ was lower than that of the BM. When the heat inputs were 2.62 and 2.45 kJ/mm, the impact toughness of the WMZ was higher than that of the BM. Therefore, α' phase was not the only factor affecting the impact toughness of the WMZ. According to the above analysis, it could be seen that the impact toughness of the WMZ could be affected by the proportion of high-angle GB and presence of α' phase.

4 Conclusions

(1) During the K-TIG welding process, 12 mm-thick TC4 titanium alloy plates were welded with varying heat inputs (2.30−2.62 kJ/mm).

(2) When the heat input gradually increased, α laths in the WMZ became fine and long, and α' phase and residual β phase were also reduced. The proportion of high-angle GBs in the WMZ also increased as the heat input increased.

(3) When the heat input was in the range of 2.30−2.62 kJ/mm, the K-TIG TC4 titanium alloy welds were well formed. The tensile strength and impact energy absorbed by the WMZ were in accordance with the welding requirements.

(4) The α' phase decreased with increasing heat input, so the tensile strength of WMZ decreased and the elongation of the WMZ increased. The impact toughness of the WMZ can be affected by the proportion of high-angle GB and the presence of α' phase.

Acknowledgments

The authors are grateful for the financial supports from the Key Research and Development Program of Guangdong Province, China (2020B090928003), the Natural Science Foundation of Guangdong Province, China (2020A1515011050), the Science and Technology Base and Talent Special Project of Guangxi Province, China (AD19245150) and Guangxi University of Science and Technology Doctoral Fund, China (19Z27).

References

[1] PENG He-li, LI Xi-feng, CHEN Xu, JIANG Jun, LUO Jing-feng, XIONG Wei, CHEN Jun. Effect of grain size on high-temperature stress relaxation behavior of fine-grained TC4 titanium alloy [J]. Transactions of Nonferrous Metals Society of China, 2020, 30(3): 668−677.

[2] YIN Mei-gui, CAI Zhen-bin, LI Zhen-yang, ZHOU Zhong-rong, WANG Wen-jian, HE Wei-feng. Improving impact wear resistance of Ti−6Al−4V alloy treated by laser shock peening [J]. Transactions of Nonferrous Metals Society of China, 2019, 29(7): 1439−1448.

[3] YANG Xin, WANG Wan-lin, MA Wen-jun, WANG Yan, YANG Jun-gang, LIU Shi-feng, TANG Hui-ping. Corrosion and wear properties of micro-arc oxidation treated Ti6Al4V alloy prepared by selective electron beam melting [J]. Transactions of Nonferrous Metals Society of China, 2020, 30(8): 2132−2142.

[4] CUI Shu-wan, SHI Yong-hua, ZHU Tao, LIU Wei-cong. Microstructure, texture, and mechanical properties of Ti−6Al−4V joints by K-TIG welding [J]. Journal Manufacturing Processes, 2019, 37: 418−424.

[5] DING R, GUO Z X. Microstructural evolution of a Ti−6Al−4V alloy during β-phase processing: Experimental and simulative investigations [J]. Materials Science and Engineering A, 2004, 365(1−2): 172−179.

[6] CUI Shu-wan, SHI Yong-hua, SUN Kun, GU Sheng-yong. Microstructure evolution and mechanical properties of keyhole deep penetration TIG welds of S32101 duplex stainless steel [J]. Materials Science and Engineering A, 2018, 709: 214−222.

[7] CUI Shu-wan, SHI Yong-hua, CUI Yan-xin, ZHU Tao. Influence of microstructure and chromium nitride precipitations on mechanical and intergranular corrosion properties of K-TIG weld metals [J]. Construction and Building Materials, 2019, 210: 71−77.

[8] CUI Shu-wan, SHI Yong-hua, CUI Yan-xin, ZHU Tao. The impact toughness of novel keyhole TIG welded duplex stainless steel joints [J]. Engineering Failure Analysis, 2018, 94: 226−231.

[9] WANG G Q, ZHAO Z B, YU B B, LIU J R, WANG Q J, ZHANG H J, YANG R, LI W J. Effect of base material on microstructure and texture evolution of a Ti−6Al−4V electron-beam welded joint [J]. Acta Metallurgica Sinica (English Letters), 2017, 30(5): 499−504.

[10] LATHABAI S, JARVIS B L, BARTON K J. Comparison of keyhole and conventional gas tungsten arc welds in commercially pure titanium [J]. Materials Science and Engineering A, 2001, 299: 81−93.

[11] ROSELLINI C, JARVIS L. The keyhole TIG welding process: A valid alternative for valuable metal joints [J]. Welding International, 2009, 23: 616−621.

[12] SQUILLACE A, PRISCO U, CILIBERTO S, ASTARITA A. Effect of welding parameters on morphology and mechanical properties of Ti−6Al−4V laser beam welded butt joints [J]. Journal Materials Processing Technology, 2012, 12(2): 427−436.

[13] ASTM International. Designation: E709—08 standard guide for magnetic particle testing [S]. West Conshohocken, PA: ASTM International, 2008.

[14] ASTM International. Designation: E8/E8M—16a standard

test methods for tension testing of metallic materials [S]. West Conshohocken, PA: ASTM International, 2016.

[15] ASTM International. Designation: A370—17 standard test methods and definitions for mechanical testing of steel products [S]. West Conshohocken, PA: ASTM International, 2017.

[16] AHMED T, RACK H J. Phase transformations during cooling in α+β titanium alloys [J]. Materials Science and Engineering A, 1998, 243: 206−211.

[17] PARK J H, HAMAD K, WIDIANTARA I P, KO Y G. Strain and crystallographic texture evaluation of interstitial free steel cold deformed by differential speed rolling [J]. Materials Letters, 2015, 147: 38−41.

[18] CUI Shu-wan, XIAN Zhi-yong, SHI Yong-hua, LIAO Bao-yi, ZHU Tao. Microstructure and impact toughness of local-dry keyhole tungsten inert gas welded joints [J]. Materials, 2019, 12: 1638.

[19] ASTM International. Designation: B256 — 05 standard specification for titanium and titanium alloy strip, sheet, and plate [S]. West Conshohocken, PA: ASTM International, 2005.

[20] WRONSKI S, TARASIUK J, BACROIX B, BACZMANSKI A, BRAHAM C. Investigation of plastic deformation heterogeneities in duplex steel by EBSD [J]. Materials Characterization, 2012, 73: 52−60.

[21] THOMAS G, RAMACHANDRA V, GANESHAN R, VASUDEVAN R. Effect of pre- and post-weld heat treatments on the mechanical properties of electron beam welded Ti−6Al−4V alloy [J]. Journal of Materials Science, 1993, 28(18): 4892−4899.

TC4 钛合金 K-TIG 焊接接头的显微组织及力学性能

崔书婉[1,2]，石永华[2]，张程士[3]

1. 广西科技大学 机械与交通工程学院，柳州 545006；
2. 华南理工大学 机械与汽车工程学院，广州 510640；
3. 柳州上汽汽车变速器有限公司，柳州 545006

摘 要：采用锁孔型钨极氩弧焊(K-TIG)在不同热量输入条件下焊接厚度为 12 mm 的 Ti−6Al−4V(TC4)钛合金板，并研究焊缝金属区(WMZ)的显微组织、晶界特征及力学性能。实验结果表明：当输入热量为 2.30~2.62 kJ/mm 时，K-TIG 焊缝成形良好，未出现明显的缺陷；当热输入逐渐增加时，α 板条的长度增加，α'相和残余 β 相减少。电子背散射衍射(EBSD)测试结果表明：WMZ 中的大角度晶界比例随着热量输入的增加而增加。当热量输入从 2.30 增加到 2.62 kJ/mm 时，WMZ 的抗拉强度逐渐降低，伸长率增加。WMZ 的冲击韧性随着热量输入的增加而增加。

关键词：K-TIG 焊接；热量输入；α'相；大角度晶界；夏比冲击断裂面

(Edited by Wei-ping CHEN)